Astron. Astrophys. 361, 529–534 (2000)

ASTRONOMY AND ASTROPHYSICS

4C 39.25: Witnessing the interaction between a moving and a stationary component

A. Alberdi[1], **J.L. Gómez**[1], **J.M. Marcaide**[2], **A.P. Marscher**[3], **and M.A. Pérez-Torres**[2,4]

[1] Instituto de Astrofísica de Andalucía (CSIC), Apartado 3004, 18080 Granada, Spain
[2] Departamento de Astronomía, Universitat de València, 46100 Burjassot, Spain
[3] Department of Astronomy, Boston University, Boston MA 02215, USA
[4] Present address: Istituto di Radioastronomia (CNR), 40129 Bologna, Italy

Received 23 May 2000 / Accepted 7 July 2000

Abstract. We present multi-epoch multi-frequency VLBI images of the compact polarized radio structure of the quasar 4C 39.25. Between 1995 and 1999, the total intensity images at 15, 22, and 43 GHz have remained almost unperturbed, while there have been significant changes in the polarized intensity maps together with a related rotation of the polarization angle. These changes in the polarized structure trace in great detail the interaction between a moving and a standing component. We interpret the stationary feature as a bend in the jet trajectory in a plane that does not contain the observer, and the moving one as a shock turning around the bend.

Key words: galaxies: individual: 4C 39.25 – galaxies: active – galaxies: jets – radio continuum: galaxies

1. Introduction

During the last 15 years several groups have performed VLBI observations of the peculiar superluminal radio source 4C 39.25 at centimeter wavelengths (e.g. Marcaide et al. 1994; Alberdi et al. 1997; and references therein). These observations revealed the presence of a superluminal component, b, moving between the western component c and the eastern component a. VLBI observations at 7mm and 1.3cm suggested the presence of a fourth, weak and inverted spectrum component d, the putative core of 4C 39.25, located $\sim$2.7 mas west of a (Alberdi et al. 1993a,b, 1997). Observations at 22, 43, and 86 GHz (Alberdi et al. 1997, 1998) suggested a spectral turnover of d between 43 and 86 GHz.

Components a and c, with steep spectra, remained constant in flux density and stationary relative to each other, while component b brightened and slowed down as it approached component a (Alberdi et al. 1993a). This result was also independently obtained by Guirado et al. (1995) and Fey et al. (1997). Guirado et al. (1995) showed, via phase-delay astrometry, that component b was moving with respect to an external reference assumed fixed while components a and c remained stationary. Moreover, Fey et al. (1997) showed that the compact extragalactic source 4C 39.25 appeared moving with respect to the radio reference frame and that such motion –as derived from the group-delay astrometric position time series– was consistent with a motion of the superluminal component b. Additionally, Fey et al. (1997) confirmed the previously reported deceleration of b (Alberdi et al. 1993a, 1997) and showed that b has stopped at the projected position of component a. Our results suggest that the interaction between a and b is taking place.

We have interpreted the parsec scale radio jet of 4C 39.25 in the framework of the relativistic jet model (e.g. Blandford & Königl 1979), adding jet curvatures to explain the coexistence of moving and stationary components (e.g. Marscher et al. 1991; Alberdi et al. 1993a, 1997, 1999; Marcaide et al. 1994). In this model, the motion and flux density evolution of component b can be explained as a shock wave travelling along a bent relativistic jet (Gómez et al. 1994). According to this model, b should continue to decelerate and to increase its flux density until it "collides" or "crosses" the area associated with component a, since it is progressively approaching to the observer's line of sight. These trends should change after the "impact".

Polarimetric observations (Alberdi et al. 1999) have shown that the polarized emission is mainly associated with the eastern part of the source (components a + b). The core d is unpolarized at high frequencies (Alberdi et al. 1999). Observations at 1.1 mm (Nartallo et al. 1998) showed polarization degrees ranging between 3.7 and 5.6% with a polarization position angle neither perpendicular nor parallel to the jet axis. At centimeter wavelengths, the degree of polarization is significantly smaller.

In this paper, we present new multi-epoch polarimetric VLBI observations of the quasar 4C 39.25 at 15, 22, and 43 GHz. As we will show, these observations trace the "collision" between a and b, and help to discriminate between different scenarios like the bent-jet model and the standing shock scenario (see below).

2. Observations and data reduction

We performed continuum polarimetric observations of 4C 39.25 with the VLBA on 19 January 1998, 29 May 1998, 25 October 1998 and 8 February 1999, each time at 15, 22, and 43 GHz. The

Send offprint requests to: A. Alberdi

data were recorded in 1-bit sampling VLBA format with 32 MHz bandwidth per circular polarization. The correlation of the data was done *in absentia* at the VLBA correlator in Socorro (NM, USA). We used the NRAO AIPS package to determine the bandpass response functions of the antennas, to correct for instrumental phase and delay offsets between the separate baseband converters in each antenna, to determine antenna-based fringe corrections and to apply the *a priori* amplitude calibration. The instrumental polarization was determined using the feed solution algorithm of Leppänen, Zensus & Diamond (1995), on the source 0420-014. Comparison with the leakage terms (D-terms) determined on the sources 4C39.25, 3C279 and OJ287 revealed a good agreement. Delay differences between the right- and left-handed systems were estimated through comparison between the VLA and VLBA polarization images of 0420-014 (Gómez et al. 2000), which were compact at both angular scales. The D-terms for all 4 epochs remained fairly constant at all frequencies. The E-vector position angles (EVPA) were determined with an error that we estimate to be within 10 degrees.

Data imaging in total intensity was performed using the Difmap package (Shepherd, Pearson & Taylor 1994). Imaging in polarized intensity was performed using the AIPS package. The January 1998 and October 1998 images have a significantly poorer quality, specially at 43 GHz, due to poor weather conditions at some of the antenna locations.

3. Results

Fig. 1 shows the VLBA total and linearly polarized intensity images of 4C39.25 at 15, 22 and 43 GHz. For comparison, we show at 15 and 22 GHz an additional image corresponding to the epoch 3 November 1995 (Alberdi et al. 1998). E-vectors are shown overlaid on the total flux density images. For each image, the maps have been aligned vertically such that the bright eastern component (component b) is at the same angular position in each image.

3.1. Total intensity images

These images confirm the previously reported parsec-scale structure of 4C 39.25: from west to east, the inverted-spectrum core d, component c which appears as a bent bridge of emission joining the core d with the superluminal component b, and the stationary component a. Components b and a are at about the same projected position. Component c has a steep spectrum and, as mentioned previously, is resolved into a bent "bridge" whose emission could be related to the underlying relativistic flow, perturbed after the passage of b. The curvature has not changed with time and does not show any frequency dependence. The 15 GHz maps are similar to those presented by Kellermann et al. (1998).

At each frequency, the intensity maps at all epochs are similar. However, the flux density associated with the a+b region is decreasing with time at all three frequencies. Such decrease can also be observed through the related decrease of the peak of brightness between Jan'98 and Feb'99: from 6.28 to 5.39 Jy/beam at 15 GHz; from 3.73 to 3.38 Jy/beam at 22 GHz; from 1.96 to 1.70 Jy/beam at 43 GHz. Model fitting of the other components show that they have mantained their fluxes through all the epochs.

The total flux density of the source at centimeter (University of Michigan data base) and (sub-)millimeter wavelengths (Teräsranta et al. 1998) decreased from 1972 to 1982, and then steadily increased until 1994, to reach its maximum value. Since this flux increase was strongly correlated with the flux increase of component b, it was interpreted as due to the motion of b along a bent path whose curvature is oriented progressively towards the observer's line of sight. Since 1994, the light curves have showed a "plateau" at this maximum and started around 1998 to decline. This behaviour is again correlated with the flux density evolution of the a+b region, probably indicating that b is already turning around a and diminishing its flux due to decreased Doppler boosting.

3.2. Polarization images

As seen in Figs. 1 and 2, the polarized emission is mainly associated with the eastern part of the source (components a and b). The core, d, and the bridge of emission, old component c, are unpolarized. Furthermore, the variability in the polarized emission is mainly due to component b. There are two systematic trends visible in Figs. 1 and 2:

(i) First, a change in the relative orientation of the polarization angles of components a and b, for each frequency, as a function of time. Such behaviour seems also consistent with integrated polarization measurements: the overall polarization angle at 15 Ghz changed from -57°$\pm$3° (1998.1) to -21°$\pm$6° (1998.41), -16°$\pm$5° (1998.75), and 26°$\pm$5° (1999.06); at 22 Ghz changed from -54°$\pm$5° (1998.1) to -17°$\pm$5° (1998.52); and at 43 GHz from -38°$\pm$6° (1998.1) to 55°$\pm$5° (1999.12). At the three frequencies, the VLBI polarized maps are mainly dominated by two sub-components with a different magnetic field orientations. The rotation is detected in the VLBI maps at all frequencies (see Figs. 1 and 2) with the easternmost polarized component polarization vector rotating clockwise. On the other hand, the westernmost polarized component shows a constant (within the errors) polarization angle.

(ii) Second, a change in the relative polarization intensities of the subcomponents that dominate the polarized maps (see Fig. 2). At the three frequencies, the ratio between the polarized intensity of the easternmost component with respect to the westernmost within the a+b complex is increasing with time. The polarized emission for the first two epochs are roughly dominated by the westernmost component, while the emission for the other two epochs – in particular for the epoch 8 Feb 1999 – becomes strongly dominated by the easternmost component. We tentatively identify the easternmost polarized component with b after passing over the westernmost polarized component a. While b is passing through a, the westernmost component dominates the polarized emission. As b passes over a, the emission of the easternmost component starts to dominate. We note that there are also some hints of small relative displacements be-

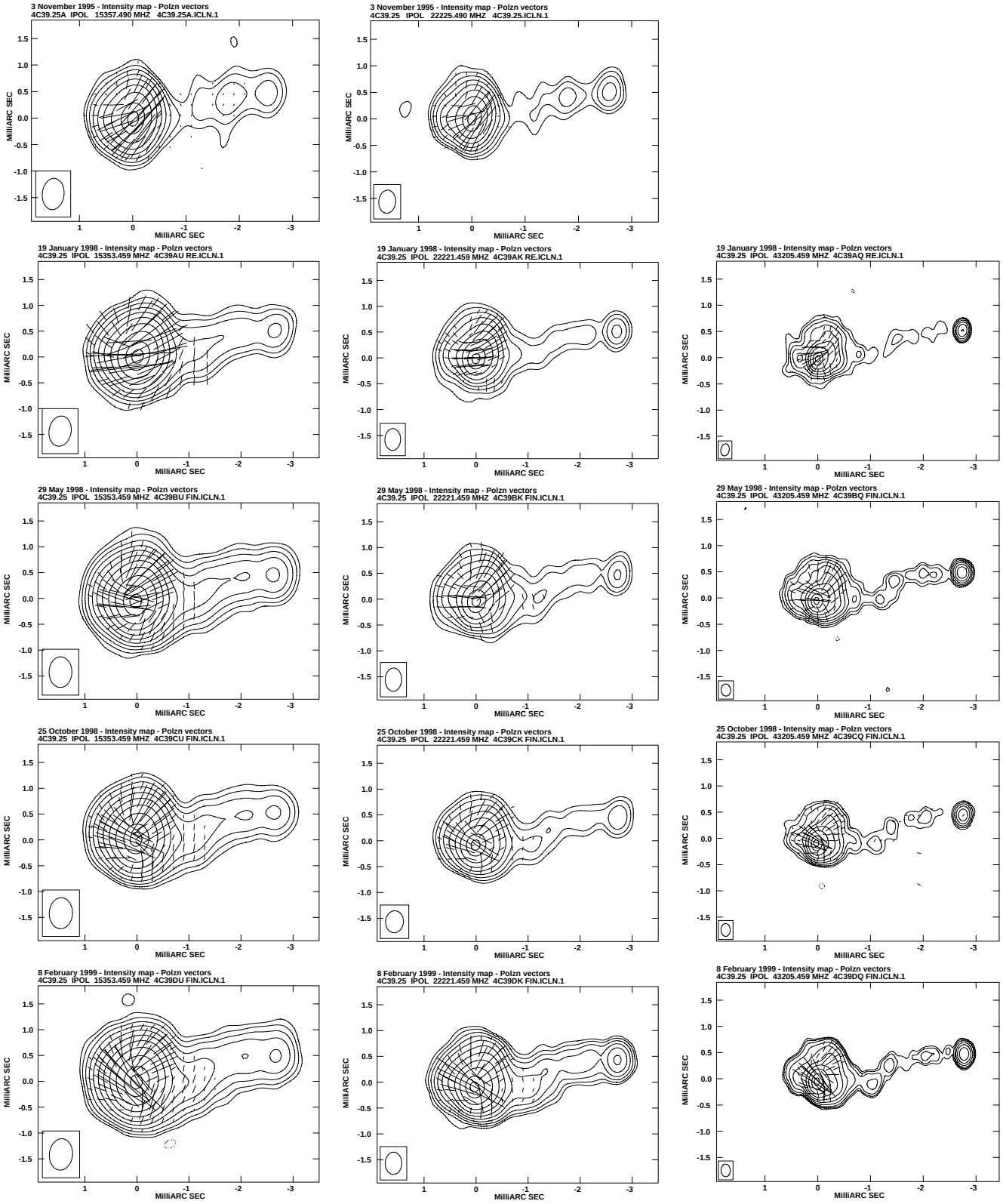

Fig. 1. Polarized flux intensity images (E-vectors with length proportional to the polarized intensity) of 4C 39.25 overlaid to the total flux density images (contours). The maps correspond (from top to bottom) to the epochs 3 November 1995, 19 January 1998, 29 May 1998, 25 October 1998, 8 February 1999 and frequencies 15, 22 and 43 GHz (from left to right). In all maps, contours are spaced by factors of $\sqrt{2}$ in brightness, with the lowest at 3 times the rms noise level. For each map we list the rms noise (mJy beam^{-1}) / the peak of brightness (Jy beam^{-1}) levels at 15, 22 and 43 GHz, respectively: *3-Nov-95:* 10.14/6.087; 6.38/3.83; *19-Jan-98:* 5.23/6.278; 6.21/3.729; 3.26/1.958; *29-May-98:* 2.59/6.218; 6.28/3.768; 1.56/1.871; *25-Oct-98:* 4.70/5.638; 5.59/3.356; 2.64/1.584; *8-Feb-99:* 2.25/5.389; 1.41/3.382; 2.26/1.693.

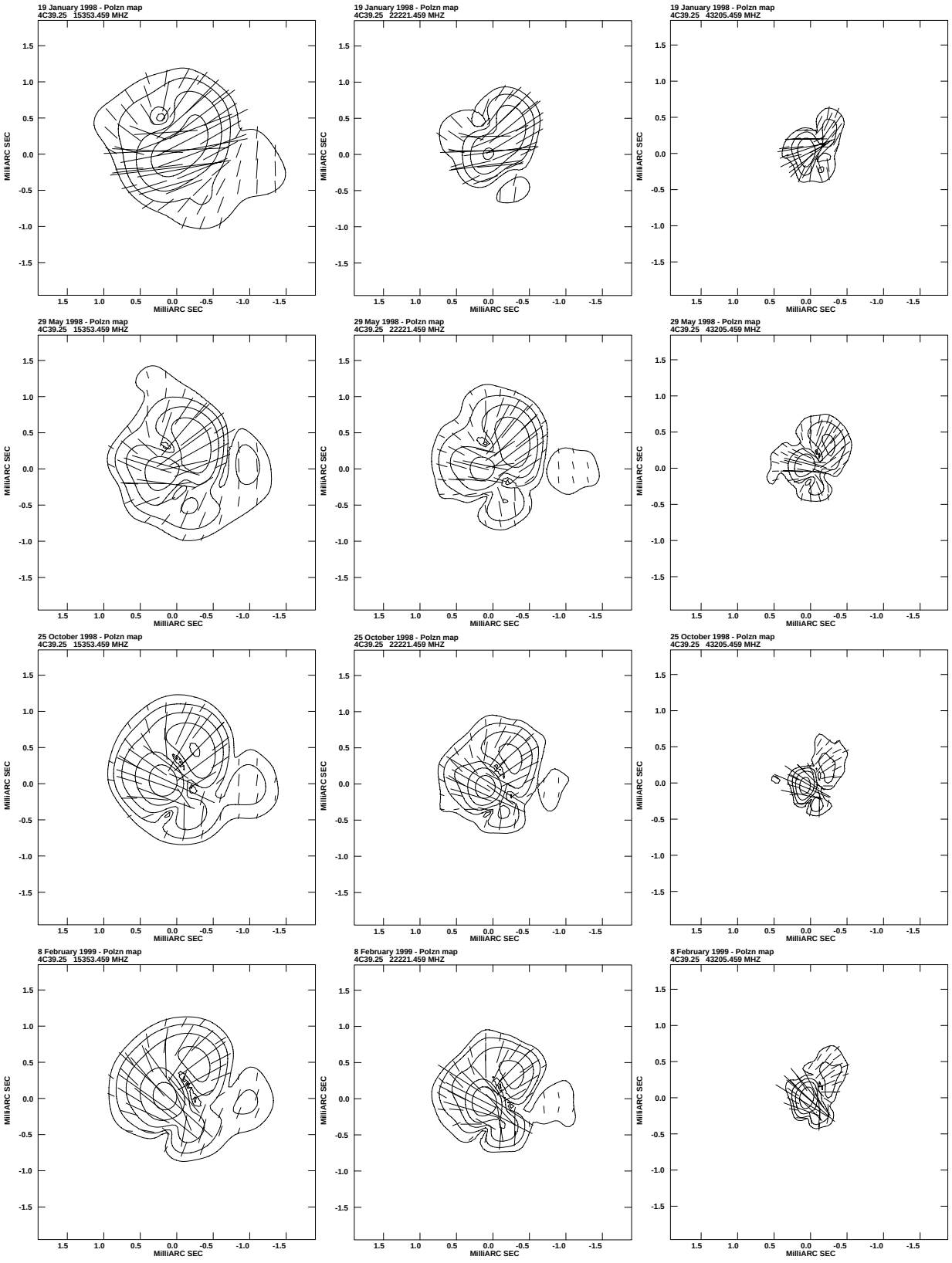

Fig. 2. Polarized flux intensity images of 4C 39.25. The maps correspond to the epochs 19 January 1998, 29 May 1998, 25 October 1998, 8 February 1999 (from top to bottom) and frequencies 15, 22 and 43 GHz (from left to right). For each map we list the rms noise (mJy beam^{-1})/the peak of brightness (mJy beam^{-1}) levels at 15, 22 and 43 GHz, respectively: *19-Jan-98:* 15/186; 15/128; 15/105; *29-May-98:* 8/118; 6/82; 10/69; *25-Oct-98:* 6/147; 6/143; 10/115; *8-Feb-99:* 8/173; 6/172; 10/135.

tween the two components, as can be inferred from the shift in the position of the minimum of polarization in the maps. These minima are clearly visible in all the maps for all frequencies and epochs (see Fig. 2).

Thus, the polarized intensity maps trace significant changes that are occuring in the source. Although components a and b are at the same projected position and are not segregated by the intensity maps, the polarized maps are showing the effects of the interaction between a superluminal component, b, and a stationary component, a, that is, the effects of a moving shock crossing a bend in the jet in a plane that does not contain the observer.

The ridge line of the jet of 4C 39.25 at parsec scales can be traced from our maps (see Fig. 3) showing the wiggles and curvatures present in the twisted jet. The observed properties of 4C 39.25 are heavily influenced by these changes in the orientation of the jet with respect to the observer, translated to the observed properties due to Doppler factor variations.

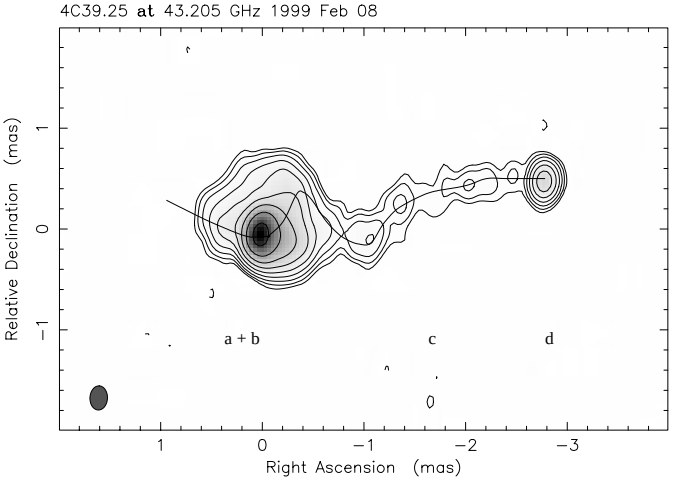

Fig. 3. Total flux intensity image of 4C 39.25 at 43 GHz with an approximate determination of the projected jet ridge line. The map correspond to the epoch 8 February 1999.

4. Discussion

Recent results have provided strong evidence in favor of an ongoing a+b interaction: i) the total flux density of 4C 39.25 is beginning to decrease at millimeter and centimeter wavelengths; ii) the polarized flux density is decreasing at centimeter wavelengths and the polarization angle rotating with time (University of Michigan database); iii) component b is decelerating at a constant rate (13.6 μas yr^{-2}) and has now practically stopped at the projected position of a (Fey et al. 1997).

Our results provide further evidence for the ongoing interaction. If we assume that the collision is occurring, the easternmost emission would correspond to the extension of b as it turns around a, and the maximum of the brightness distribution corresponds to the interacting components a+b seen in projection. Several strong arguments give support to this scenario:

i) The light curve of 4C39.25 suffered an impressive and monotonic increase from 1984 to 1994: at 3.6cm, it increased from $\sim$5 Jy to $\sim$14 Jy (University of Michigan database); at 1.3cm, from $\sim$3 Jy to $\sim$12 Jy (this paper and Teräsranta et al. 1998); at 37 GHz, from $\sim$2 Jy to $\sim$ 10 Jy (Teräsranta et al. 1998). This increase is associated with the flux density increase of component b, which represents the strongest shock ever reported in the literature for a parsec-scale radio jet. From 1996 on, the light curves have reached a plateau and are now decreasing very slowly;

ii) the global size of the milliarcsecond structure of 4C 39.25 has increased (angular size $\geq$3.0 mas) with respect to previously reported epochs (angular size 2.7$\pm$0.2 mas; Marcaide et al. 1994; Alberdi et al. 1993a, 1997, 1998). This could be explained if the eastern limb of b has already passed over the region associated with the stationary component a;

iii) time delay effects in highly relativistic jets well aligned with the observer explain naturally the lengthening of b (Gómez et al. 1994). Due to the time delay, as the shock travels along the bent jet (see Fig. 3), the shock front rotates, becoming almost parallel to the line of sight (LOS), and the length of the shocked region increases when viewed in the observer's frame. This effect depends strongly on the jet orientation with respect to the LOS and causes an enhancement of the emission;

iv) the total flux density maps are very similar for all epochs. While b is turning around a, the source structure will look rather similar due to projection effects, but the flux density of the region will decrease slowly, but steadily;

v) the polarized flux density maps change dramatically; considering that the shocks enhance the component of the magnetic field parallel to the shock front and that the unperturbed magnetic field is mainly random, the rotation of the polarization vectors would mark and trace the projected bend in the jet trajectory (see Fig. 3) as it turns away from the observer. This scenario would require a bend in a plane that does not contain the observer. In this case, and assuming an angle to the LOS of $\sim 7^\circ$ (Alberdi et al. 1993a), the rotation of the polarization angle would imply a deprojected rotation angle larger than 5°. This rotation is consistent with the strengthening in polarized flux of the easternmost component with time: the degree of polarization is increasing as the jet is turning away from the observer (for the case of a jet aligned to the LOS and a component with its magnetic field perpendicular to the jet, the degree of polarization is negligible). Moreover, this rotation is also consistent with the slight decrease in the total intensity brightness maximum, due to a decrease in the Doppler-boosting of the radiation intrinsic to component b.

We conclude that b is emerging from the downstream side of a. Our data confirm our previous model (Alberdi et al. 1993a) of a being a stationary feature where the jet bends towards the line of sight and b a superluminal component passing through it.

We can predict the future evolution of the parsec-scale: component b will leave the region where the emission from component a originates with a monotonically increasing proper motion and a monotonically decreasing flux density. The specific evolution of the proper motion, total and polarized intensity

light curves, and polarization angle will depend on the –still unknown– jet geometry eastwards of component a. We expect the motion of component b to be along a direction approaching the one of the kiloparsec-scale structure (P.A. $\sim 78^\circ$, Jackson et al. 1993).

We can postulate a possible recurrent ejection of a new component, let us call it e, from the core component d as already suggested by Marcaide et al. (1989). In such case, we should eventually see a strengthening of the bridge component c, followed by the superluminal motion of the new component e between c and a. There are already some hints to support our conjecture, since the source structure at the epochs presented in this paper looks very similar to that of the August 1973 $\lambda 3.6$ VLBI image (Baath et al. 1980), being the source structure dominated by the easternmost component (in 1973 the light curve reached a maximum with a flux density of ~ 11.2 Jy at 8.4 GHz); after a decrease through 1984 and a new increase, the light curve reached a new maximum in 1994 of ~ 14 Jy, decreasing very slowly from then on (~ 13.1 Jy in Feb. 1999; University of Michigan database). This conjecture was already advanced by Marcaide et al. (1989). If now the conjecture turns to be true, we should now expect a source evolution similar to the one between 1973 and 1984.

An alternative interpretation for our observations, that we consider less plausible, is that the standing component, a, is a recollimation shock (Gómez et al. 1997) and the superluminal component, b, is a moving shock travelling through it. According to this interpretation, component a (the easternmost component), is polarized at all three frequencies with the E-field aligned along the jet axis (B-field perpendicular) due to the compression produced by the recollimation shock (Komissarov et al. 1997). The superluminal component b, interpreted as a shock moving down the jet, is also polarized: its magnetic field is not perpendicular to the jet axis, suggesting that the shock is oblique (Cawthorne & Cobb 1990), or the B-field is following the bent trajectory of the jet in this region of the source (Gómez et al. 1994). The similarity of all the total intensity maps argues in favour of this option, but the drastic changes in the polarized intensity maps seems to exclude this interpretation.

5. Conclusions

We present results from four epochs of multi-frequency observations of the parsec-scale radio jet of 4C 39.25 on 1998 and 1999. Our observations provide evidence for an ongoing interaction between a superluminal component and a stationary component. Although the total intensity images are very similar at all epochs, the polarization images show drastic changes with time: a progressive rotation of the E-vectors at all frequencies and related changes in the polarized intensity. We conclude that the eastern limb of the superluminal component has already passed over the region associated with the stationary component and is now changing its orientation away from the observer. A source model of a stationary feature where the jet bends into the line of sight and a shock passing through it is consistent with the data.

Acknowledgements. This research is supported in part by the Spanish DGICYT, under grant PB97-1164. It has made use of data from the University of Michigan Radio Astronomy Observatory which is supported by funds from the University of Michigan. The National Radio Astronomy Observatory is a facility of the National Science Foundation operated under cooperative agreement by Associated Universities, Inc.

References

Alberdi A., Marcaide J.M., Marscher A.P.,. et al., 1993a, ApJ 402, 160
Alberdi A., Krichbaum T.P., Marcaide J.M., et al., 1993b, A&A 271, 93
Alberdi A., Krichbaum T.P., Graham D.A., et al., 1997, A&A 327, 513
Alberdi A., Lara L., Gómez J.L., et al., 1998, In: Zensus J.A., Taylor G.B., Wrobel J.M. (eds.) Radio Emission from Galactic and Extragalactic Compact Sources. IAU Coll. 164, ASP Conference Series Vol. 144, p. 115
Alberdi A., Gómez J.L., Marcaide J.M., et al., 1999, New Astronomy Reviews 43, 731
Baath L.B., Cotton W.D., Counselman C.C., et al., 1980, A&A 86, 364
Blandford R.D., Königl A., 1979, ApJ 232, 34
Cawthorne T.V., Cobb W.K., 1990, ApJ 350, 536
Fey A.L., Eubanks M., Kingham K.A., 1997, AJ 114, 2284
Gómez J.L., Alberdi A., Marcaide J.M., Marscher A.P., Travis J., 1994, A&A 292, 33
Gómez J.L., Martí J.M., Marscher A.P., Ibañez J.M., Alberdi A., 1997, ApJ 482, L33
Gómez J.L., et al., 2000, in preparation
Guirado J.C., Marcaide J.M., Alberdi A., et al., 1995, AJ 110, 2586
Jackson N., Browne I.W.A., Alberdi A., Marcaide J.M., 1993, A&A 280, 128
Kellermann K.I., Vermeulen R.C., Zensus J.A., Cohen M.H., 1998, AJ 115, 1295
Komissarov S.S., Falle S.A.E.G., 1997, MNRAS 288, 833
Leppänen K.J., Zensus J.A., Diamond P.J., 1995, AJ 110, 2479
Marcaide J.M., Alberdi A., Elósegui P., et al., 1989, A&A 211, L23
Marcaide J.M., Alberdi A., Gómez, J.L., Guirado J.C., 1994, In: Zensus J.A., Kellermann K.I. (eds.) Compact Extragalactic Radio Sources. NRAO-AUI, p. 141
Marscher A.P., Zhang Y.F., Shaffer D.B., Aller H.D., Aller M.F., 1991, ApJ 371, 491
Nartallo R., Gear W.K., Murray A.G., et al., 1998, MNRAS 297, 667
Shepherd M.C., Pearson T.J., Taylor G.B., 1994, BAAS 26, 987
Teräsranta H., Tornikoski M., Mujunen A., et al., 1998, A&AS 132, 305